Energy Selection Functions: Modelling the Energetic Drivers of Animal Movement and Habitat Use

by

Natasha Jean Klappstein

A thesis submitted in partial fulfillment of the requirements for the degree of

Master of Science

in

Ecology

Department of Biological Sciences

University of Alberta

Abstract

Energetics are a key driver of animal decision-making, as survival depends on the balance between foraging benefits and movement costs. However, this fundamental perspective is often missing from habitat selection studies, which mainly describe correlations between observed space use and environmental features, rather than assessing the mechanisms behind these correlations. To address this gap, we present a new model, the energy selection function (ESF), to assess how moving animals choose habitat based on energetic considerations, thus incorporating a key aspect of evolutionary behaviour into habitat selection analysis. The ESF provides a way to test foraging and movement hypotheses, by evaluating selection for energetic gains and costs. In this thesis, we contrast the ESF to other habitat selection models, provide guidelines for defining energetic covariates, and demonstrate the model's utility with simulations and a case study of polar bears. Simulations indicate that the ESF can be fitted with low estimation errors, under a number of modelling choices and biological scenarios. Our case study shows how cost-minimization may arise in species that inhabit environments with an unpredictable distribution of energetic gains. Because of its close links to existing habitat selection models, the ESF is widely applicable to any study system where energetics can be derived, and has immense potential for methodological extensions.

Preface

This thesis is my original work, but was conducted as part of an international collaboration. The initial idea for the model was conceived by J.R. Potts (University of Sheffield, UK) and L. Börger (Swansea University, UK), and the application to polar bears was led by myself and A.E. Derocher. The collaboration grew to include T. Michelot (University of St Andrews, UK) during a 2019 research visit in the UK. The seal data in section 4 was produced by N.W. Pilfold (San Diego Zoo, USA) and A.E. Derocher provided the polar bear telemetry data. I led the project development, and conducted the analysis, with assistance from T. Michelot and input from all collaborators and my supervisory committee. I wrote the thesis and the associated manuscript.

A modified version of this thesis is currently under review at *Ecology Letters* as: Klappstein NJ, JR Potts, T Michelot, L Börger, NW Pilfold, M Lewis, & AE Derocher. "Energy selection functions: modelling the energetic drivers of animal movement and habitat use" and is available as an Authorea preprint with the same name.

To Théo and Jeffrey,

For making every failure bearable and every success even more rewarding.

Acknowledgements

My time in this MSc has been truly amazing. I have been fortunate enough to tag polar bears in Manitoba and conduct research in the UK. I am grateful for funding from the Northern Scientific Training Program and Mitacs Globalink that made these experiences possible.

There are many people who directly contributed to this thesis. A huge thank you to my supervisor, Dr. Andrew Derocher, for his ongoing support. Despite some blemishes on my transcript, Andy believed in my potential as a scientist and guided me through this process. Andy's motive has always been to ensure my success, and we have had many tremendously helpful discussions about my scientific aspirations and trajectory. Also, thank you to Dr. Mark Lewis for serving on my supervisory committee and being involved in a larger capacity than required. I would like to acknowledge the contributions of all my collaborators who worked on this project from afar: Drs. Jonathan Potts, Luca Börger, Théo Michelot, and Nick Pilfold. It has been very rewarding to work with you and I hope to again in the future.

I am grateful to everyone that made my MSc so memorable, educational, and fulfilling. I want to thank David McGeachy for the incredible field experience in September 2018; this "fair-weather bear-tagger" won't soon forget it. Thank you to those who patiently taught me important field skills (David, Andy, Dr. Nicholas Lunn), including "never sit directly at the back end of an anaesthetized polar bear". Regarding the analytical component of my thesis, I greatly appreciate the quantitative scientists (Jonathan, Mark, Théo) that took the time to discuss difficult modelling questions with me, with no judgement of my in-progress statistical competency. Also, a special thank you to Ron Togunov. You have been absolutely instrumental in my development as a scientist and you have been a consistent and tremendous source of support. I truly value our science talks, side projects, and friendship.

I'm *incredibly* grateful for the support and love from my parents, my son, and my partner. I was a single parent for most of my time in university, and would not have finished two degrees without the (seemingly limitless) help from my parents. Thank you to my son,

Jeffrey, for being my motivation and my reality check when I was consumed by the stress of classes and research. Finally, Théo: you began as a collaborator and since have become my best friend and partner in life. I am grateful for everything from whiteboard talks on habitat selection, to hiking in the mountains (far, far away from work), and everything in between.

Contents

List of Figures

1 Introduction

Foraging and movement are core considerations in animal ecology that reflect fundamental aspects of energetic balance and optimality. Animals should distribute themselves in space so as to maximize their access to energetically rich resources, while minimizing the costs of travel associated with foraging (Emlen, 1966; MacArthur & Pianka, 1966; Pyke *et al.*, 1977; Pyke, 2019). Therefore, energetic balance is a critical component of optimal foraging theory, which assumes that foraging animals should maximize their net energy intake. Theories of how animals search for and distribute themselves relative to food range from random search strategies (Shlesinger & Klafter, 1986; Viswanathan *et al.*, 1999; Bartumeus & Catalan, 2009) to cognitively-based movement decisions (Charnov, 1976; Pyke *et al.*, 1977; Pyke, 2019). However, many of these models are based on unrealistic assumptions that animals have either no knowledge (e.g., Lévy foraging) or perfect knowledge (e.g., cognitive foraging theory) of their environmental surroundings and internal state (Pyke, 2015, 2019). In response to these limitations, there has been increased interest in modelling the mechanistic processes of foraging movement (Nathan *et al.*, 2008; Pyke, 2019). While these models have considered the role of memory and perception in foraging (Van Der Post & Semmann, 2011; Bonnell *et al.*, 2013), attempts to estimate the direct energetic consequences of movement decisions are still rare. Energy-based models could provide a crucial link between movement and foraging ecology, uniting them under a common bioenergetic paradigm.

Optimal foraging research often focuses on the energetic benefits of movement and space-use patterns. These studies successfully describe foraging strategies in a patchy environment, and examine prey and patch selection based on factors such as travel time, perception, and memory (Charnov, 1976; Van Der Post & Semmann, 2011; Bonnell *et al.*, 2013). To assess food preference, habitat selection models often include covariates that represent foraging potential. These covariates are usually approximate measures of forage quality or resource availability (e.g., Hansen *et al.*, 2009; Bastille-Rousseau *et al.*, 2020), but may not be proportional to energetic benefits. Even in cases with more realistic depictions of energy intake (e.g., the energetic profitability of resources combined with biomass; Fortin *et al.*, 2003), the role of energetic costs is still often unquantified. Therefore, although these studies have been instrumental to understand resource preference, new models with realistic depictions of energy could be useful to better understand the mechanisms of animal space use.

When considered in a foraging context, energetic costs are often assumed to increase linearly with time and/or distance (Reynolds, 2013). In reality, the costs vary widely depending on factors such as mode of transport (Nathan *et al.*, 2008; Griffen, 2018) and environmental conditions (e.g., topography, weather, substrate) (Crête & Larivière, 2003; Wilson *et al.*, 2012). Energy landscapes have been developed as a method to evaluate environmentally-varying movement costs, which can be combined with animal movement data (Wilson *et al.*, 2012; Shepard *et al.*, 2013; Gallagher *et al.*, 2017). Environmental variables, such as air velocity for birds (Shepard *et al.*, 2013), water depth for diving animals (Wilson *et al.*, 2012), or habitat type (Pagano *et al.*, 2020), may be considered in cost estimations. Since energy landscapes are based on spatiotemporal environmental data, these models quantify the energetic costs of moving through heterogeneous or dynamic environments and could be powerful if combined with foraging theory.

To link foraging and movement, optimality models should quantify both the energetic costs and gains of movement decisions. Despite long-standing interest in cost-benefit functions (Schoener, 1971; Sih, 1984), there have been few attempts to energetically compare movement costs to the associated nutritional benefits (Nathan *et al.*, 2008; Owen-Smith *et al.*, 2010). As foraging theories are ultimately interested in energy, we propose using bioenergetics as a unifying currency in movement decision-making. With this approach, we can assess the relative contribution of energetic gains and costs to observed movements. Animals may make movement decisions primarily based on the need to maximize energy intake, minimize energy use, or balance the two (Schoener, 1971; Shepard *et al.*, 2009). By examining energetics at the scale of movement steps (i.e. movements between successive recorded locations), we can link movement ecology to its energetic drivers, allowing us to assess support for foraging theories. We can therefore gain insights into how energetic trade-offs give rise to movement and space-use.

In this paper, we introduce a method that explicitly considers movement and habitat selection in an energetic context. In a model we term an energy selection function (ESF), we evaluate preference for energetic covariates, representing energy gain and energy expenditure. We describe the methodological links to resource and step selection functions (RSFs, SSFs), while showing how the ESF is conceptually unique in its treatment of movement and habitat availability. We provide practical guidance to implement the ESF and define covariates, verify the inference procedure through simulations, and provide an example case study of

polar bears (*Ursus maritimus*) in the Beaufort Sea, Canada.

2 The ESF

2.1 ESF Model Formulation

We first present standard habitat selection models (RSFs, SSFs) from which we base the ESF. To estimate habitat preference, these models employ a use-availability approach, in which we contrast where the animal went (i.e., what resources they used) with where they could have gone (i.e., available habitat) (Manly *et al.*, 2002; Fortin *et al.*, 2005). While RSFs assess habitat selection at the scale of the utilization distribution (Manly *et al.*, 2002), SSFs are used to analyze autocorrelated animal tracking data and describe resource preference at the scale of the movement step (Fortin *et al.*, 2005; Forester *et al.*, 2009; Thurfjell *et al.*, 2014). SSFs consider that movement constraints limit the habitat availability of an RSF, and give the likelihood of a movement step ending at location y given that it started at location x in the study region Ω as

$$f(y|x) = \frac{\Phi(y|x)w(x,y)}{\int_{z\in\Omega}\Phi(z|x)w(x,z)dz}. \tag{1}$$

Following Forester *et al.* (2009), we consider the numerator to be the SSF. The first term, $\Phi(y|x)$, is the resource-independent movement kernel, which describes how an animal would move in a homogeneous landscape or in the absence of resource preference (Forester *et al.*, 2009). The second term, $w(x,y)$, is a weighting function and represents resource selection without movement constraints (i.e., if $\Phi(y|x)$ is uniform over Ω). The weighting function is typically defined as a log-linear model: $w(x,y) = \exp\{\beta \cdot H(x,y)\}$, where β is a vector of parameters representing the strength of selection for $H(x,y)$, a vector of habitat covariates. Therefore, by assuming the step density to be a product of resource selection $w(x,y)$ and movement $\Phi(y|x)$, SSFs consider the effect of environmental covariates on short-term movement decisions. The denominator of Equation 1 is a normalization constant that ensures the SSF likelihood is a probability density function with respect to y (Forester *et al.*, 2009; Potts *et al.*, 2014). The likelihood can be optimised with respect to β, over all steps, to estimate the set of parameters that maximise the likelihood of an animal selecting the used locations relative to the rest of the available habitat.

We present the ESF as an energy-based habitat selection model. The mathematical formulation is similar to a standard SSF, and it employs many of the same modelling approaches. Broadly, the ESF can be viewed as a special case of SSF, where the resource independent movement kernel is uniform over the whole study region, and where the covariates are based on energetic currencies. The ESF defines the likelihood of a step ending at location y given that it started at location x as

$$f(y|x) = \frac{w(x,y)}{\int_{z\in\Omega} w(x,z)dz}, \tag{2}$$

with energy preference modelled as,

$$w(x,y) = \exp\{\beta_1 G(x,y) - \beta_2 C(x,y)\}. \tag{3}$$

We hereafter refer to equation 3 as the ESF, where $G(x,y)$ and $C(x,y)$ refer to the energetic gain and energetic cost of the step, respectively. These energetic covariates replace the typical habitat covariates $H(x,y)$ used in SSFs, allowing us to make inferences about the role of energy in shaping movement. In section 2.3, we explain how energetic covariates can be derived from various types of telemetry and environmental data. In this form, β_1 represents the selection for energetic gains $G(x,y)$, which may be formulated in terms of energetically beneficial resources, whereas β_2 represents the strength of selection against energetic costs, which may reflect avoidance of costly movements and environments. When evaluated together, these parameters provide inferences about different energy maximization strategies in optimal foraging theory.

In the ESF, we do not need to include the resource-independent movement kernel $\Phi(y|x)$ as a separate term. Rather, since the various aspects of animal movement, such as speed and tortuosity, directly affect energy expenditure (Halsey, 2017; Wilson *et al.*, 2020), they are therefore accounted for in the cost term, $C(x,y)$. We illustrate how movement can be incorporated into $C(x,y)$ in Figure 1, which shows how energetic gains and costs contribute to the ESF. Thus, similarly to integrated step selection analysis (iSSA; Avgar *et al.*, 2016), the ESF can be viewed as evaluating movement and habitat selection simultaneously.

2.2 Implementation

Consider a movement track $\{x_1, x_2, ..., x_n\}$ collected at regular time intervals. The ESF defines the likelihood of the entire track as $L(\beta_1, \beta_2 \mid x_1, ..., x_n) = \prod_{i=1}^{n-1} f(x_{i+1}|x_i)$, where

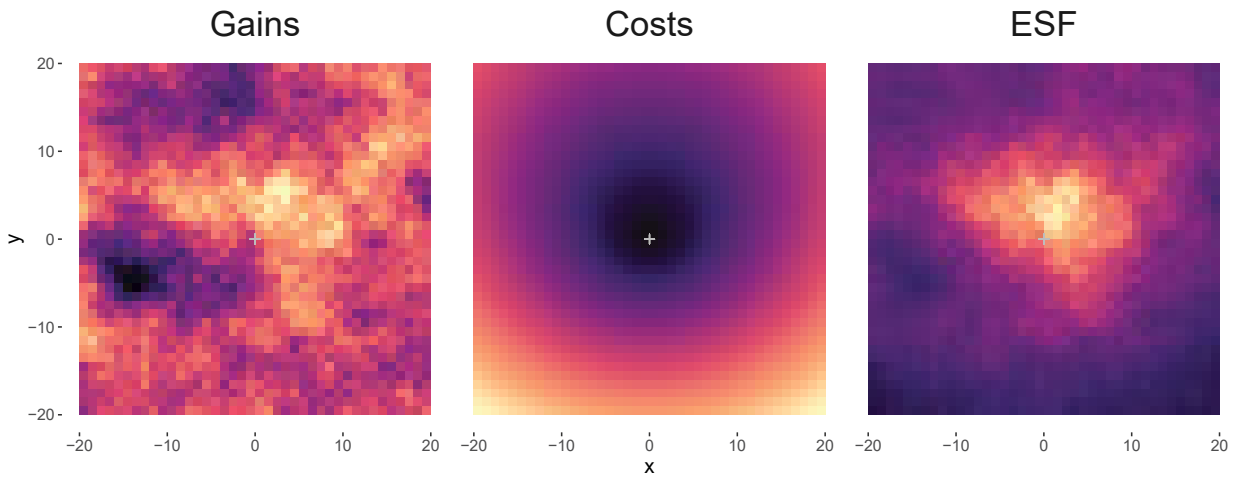

Figure 1: Simulated rasters of energetic gains and energetic costs, and the corresponding ESF. Energetic gains were simulated as a random covariate field and energetic costs were defined as a product of the step length and turning angle from the central location (+), assuming that the animal was facing up the y-axis before turning. $ESF = \exp(gains - costs)$ to represent optimal movement. In all panels, lighter colours represent higher values.

$f(x_{i+1}|x_i)$ is the likelihood of a single step (equation 2). However, it can be computationally demanding to calculate the exact likelihood, as this would require evaluation of w over the entire domain of integration Ω (i.e., continuously over the whole study region). This is a standard problem in other habitat selection studies (RSFs, SSFs), as the integral may be intractable (Rhodes *et al.*, 2005) or require computationally demanding, and possibly unreliable, numerical integration methods (Forester *et al.*, 2009). In practice, we can approximate this likelihood using a case-control design (Forester *et al.*, 2009; Thurfjell *et al.*, 2014). For each observed location x_i (hereafter, a case), we generate a set of random locations (hereafter, controls) which represent a sample of the available habitat. Using Monte Carlo integration over the control locations $\{z_{i1}, z_{i2}, ..., z_{iK}\}$, we calculate the approximate likelihood as

$$\tilde{L}(\beta_1, \beta_2 | x_1, ..., x_n) = \prod_{i=1}^{n-1} \frac{w(x_i, x_{i+1})}{\sum_{k=1}^{K} w(x_i, z_{ik})}. \tag{4}$$

In theory, we should generate control locations $\{z_{i1}, z_{i2}, ..., z_{iK}\}$ uniformly across the whole habitat Ω. This procedure would be computationally intensive, but it can be improved by noticing that the ESF (equation 3) will typically take small values over most of Ω. That is, the properties of energetic costs ensure that the ESF decays as a function of the distance

to the start point of the step x_i (see Appendix 1 for further explanation and evaluation of this concept). It is therefore sufficient to evaluate the ESF over a neighbourhood of the start point, and we suggest generating control locations uniformly on a disc around x_i. Practically, this is the same as Arthur *et al.* (1996), but is conceptually different. The radius R of the disc needs to be large enough, such that the probability of the animal moving beyond R is negligible. This sampling is not a model of movement or availability, unlike SSFs where controls are distributed according to $\Phi(y|x)$. We suggest using control locations over a disc merely for computational convenience, and in the ESF framework, the availability is determined by the effect of energetic costs on movement.

Given that the ESF uses the same general formulation and case-control design as SSFs, model fitting can be done using the same statistical techniques and software. We can estimate β_1, β_2 with maximum likelihood estimation (MLE), with regards to equation 4. MLE is fast and accessible, using numerical optimizers (e.g., *optim* in R) or existing software for conditional logistic regression (e.g., the R function *clogit*, package *survival*). The ESF may be appealing to practitioners, as it builds on existing models and can be implemented with common software and techniques.

2.3 Defining the Energetic Covariates

The energetic covariates, G (gains) and C (costs), must be formulated specifically to each study. Generally, both energetic gains and energetic costs may be defined in terms of movement and habitat covariates, although the contribution of each varies between G and C (Figures 1, 2; energetic gains will mostly depend on resources and energetic costs on movement). In this section, we provide some general recommendations on how to define G and C, although these may not be applicable to every system. In practice, the formulation of G and C should be based on available ecological knowledge, data, and expert opinion.

Energetic Gains, G

Energetic gains arise from the consumption of energetically beneficial resources, whose distribution can be derived from environmental data (Figure 2a). Wherever possible, metrics used in G should be proportional to energy (e.g., biomass is preferable to a relative habitat quality index). Further, G can incorporate multiple resources, combined by their energetic contribution (e.g., several vegetation types, weighted based on their energy content). Un-

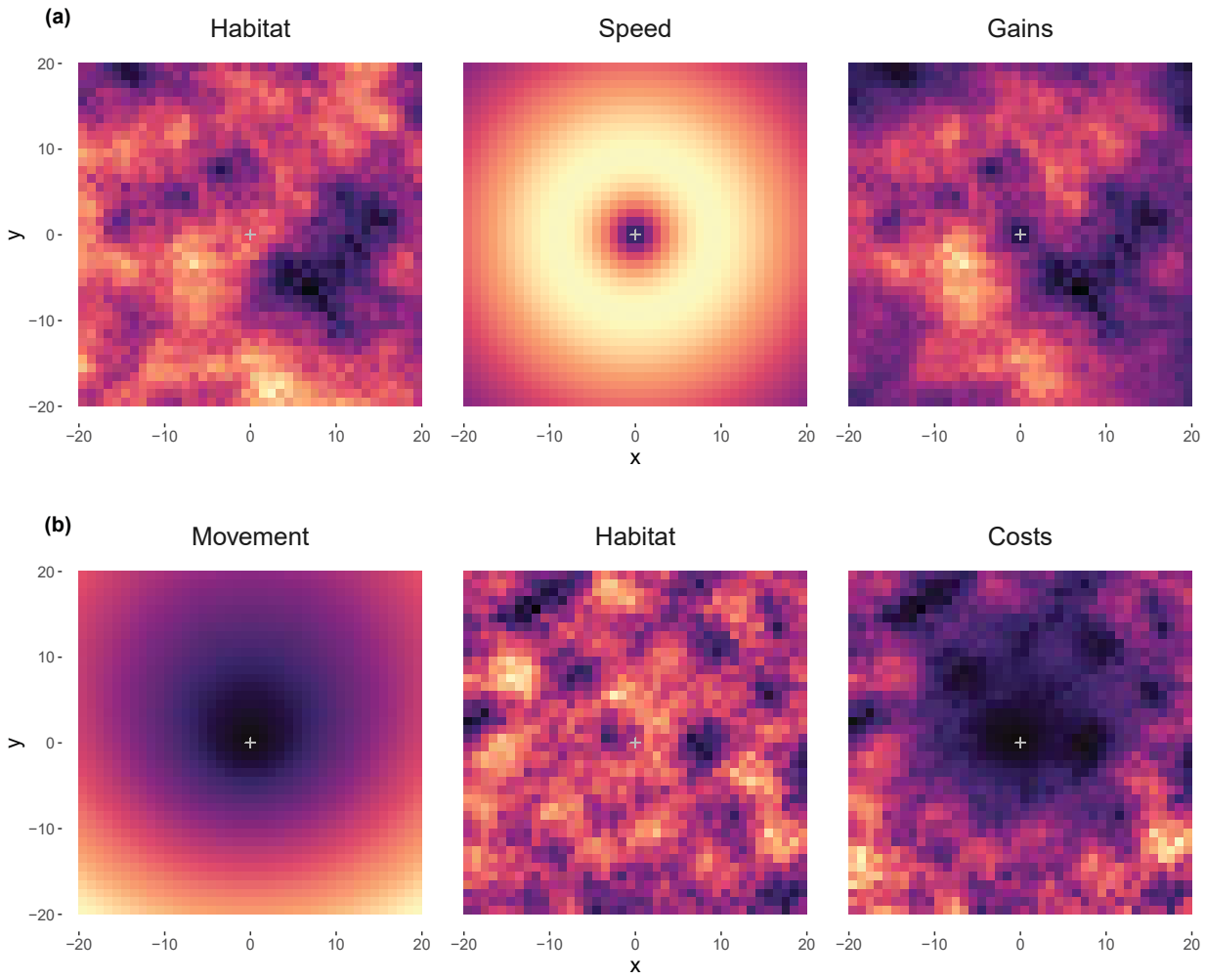

Figure 2: Example energetic gain G (a) and energetic cost C (b) formulations. In all panels, higher values are lighter in colour. In both (a) and (b), the third panel is a product of the first two panels, which represent movement and habitat components. In (a), energetic gains are composed of an energetically beneficial habitat covariate (e.g., forage biomass) scaled to the speed travelled. In this case, the effect of movement speed is gamma distributed ($k = 2$, $\theta = 2.2$) about the start point to represent decreased foraging potential at low and high speeds. In (b) the energetic costs are defined by the distance and turning angle from the start point (+; assuming movement up the y-axis), combined with a habitat covariate in which higher values increase energy expenditure.

der this formulation, we evaluate selection for all foraging resources as a single energetic currency, rather than preference for individual resources.

Additionally, energetic gains may depend on the speed travelled by the animal. For example, grazing herbivores travelling at slow speeds may deplete resources along their path, while fast travel leaves no time for foraging. In such a case, we may assume a non-linear relationship where energetic returns are lower at very low and high speeds (Figure 2a). However, for some species the relationship may be unclear or highly variable. Some predators may employ both ambush and active hunting (Higginson & Ruxton, 2015), and it may be unclear how their movement speed affects prey capture rate. Therefore, scaling gains based on movement should only be done when there is considerable empirical or theoretical support for hypothesized relationships.

Energetic Costs, C

Generally, energy expenditure will increase with movement speed (Taylor *et al.*, 1970) and tortuosity (Wilson *et al.*, 2013; Halsey, 2016; McNarry *et al.*, 2017), and with habitat factors, such as environmental softness (Crête & Larivière, 2003), slope (Halsey, 2016), and resistivity (e.g., wind and water currents; Chapman *et al.*, 2011; Shepard *et al.*, 2013). Field metabolic rates of free-ranging animals can be measured with several methods, such as doubly-labelled water, heart rate sensors, and accelerometers. Doubly-labelled water provides an accurate measure of energy use, conceptually similar to oxygen consumption, but is logistically difficult (Nagy, 1989; Speakman, 1997; Butler *et al.*, 2004; Pagano & Williams, 2019). A more practical alternative is to estimate energy expenditure using biologgers (e.g., heart rate sensors, accelerometers), calibrated using captive surrogates (Pagano & Williams, 2019; Wilson *et al.*, 2020). These tags can be fitted to animals over longer periods of time, and when combined with location data, encompass the effects of both movement and habitat. Energy expenditure estimated from observed steps can therefore be correlated to movement and habitat characteristics, and these relationships can be used to calculate the costs of control steps in the ESF (Figure 2b).

A similar approach could be used when only two-dimensional geographical positioning system (GPS) location data is available. That is, it may be possible to use metabolic rates estimated from doubly-labelled water and biologgers to model the costs of observed GPS tracks (as done with control locations, described above). In cases where this data

is unavailable, other sources of energetic information (e.g., treadmill studies) can create a synthetic model of energy expenditure. The options to do this will vary depending on the species, and should be done cautiously, as captive studies often underestimate field metabolic rates (Bidder *et al.*, 2017). Ultimately, the energy cost model should incorporate movement and habitat in a way that it is applicable to both observed and control steps.

3 Simulation Study

We ran simulations to assess the performance of the ESF inference method (section 2.2). The main objective was to recover model parameters from movement tracks simulated directly from the ESF, with known parameter values. For all simulations, G was defined as a random covariate field and C was calculated as the step length, both from $[0, 1]$ and assumed to be in the same units.

3.1 Methods

Simulation Algorithm We generated n locations $x_1, x_2, \ldots, x_n$, with x_1 selected randomly from the study area Ω. For each iteration $i = 1, \ldots, n-1$, we followed these steps to generate x_{i+1}:

1. Simulate possible endpoints $\{z_1, z_2, \ldots, z_K\}$ uniformly on a disc centred on x_i, with a radius $R = 1$.

2. Evaluate G and C at each endpoint.

3. For $k \in 1, 2, ...K$, sample x_{i+1} from $\{z_1, z_2, \ldots, z_K\}$, with probabilities defined by

$$p_k = \frac{w(x_i, z_k)}{\sum_{j=1}^{K} w(x_i, z_j)}, \tag{5}$$

   where w is the ESF (Equation 3).

Simulation Scenarios First, we assessed whether the true selection strength affected our ability to estimate the parameters, and subsequently, whether certain foraging strategies may be harder to identify. For both β_1 and β_2, we considered 15 as a high parameter value. We considered low parameter values to be 0 for β_1 (no selection for gains), and 5 for β_2 (very weak selection against costs). We could not use 0 for β_2, as the ESF simulation algorithm would

artificiality constrain the step length to be smaller than the samoling radius R. We tested different values of β_2 and found that 5 was the lowest parameter value where the size of the radius no longer had a substantial effect on the simulated step lengths. We combined these parameter values to represent the following movement patterns: i) optimal movement (high values of both parameters), ii) intake maximization (high β_1, low β_2), iii) cost minimization (low β_1, high β_2), and iv) movement nearly free of energetic considerations (low values of both parameters). Next, we altered the level of spatial autocorrelation in G. We simulated the study area Ω as a 1000×1000 raster with a resolution of 0.25, and assigned each grid cell a random value [$\sim U(0, 1)$]. We calculated the covariate field for G by using a circular moving average window with diameter ρ (measured in grid units) to control the degree of spatial autocorrelation (Avgar *et al.*, 2016; Michelot, 2019). We created random rasters of G with $\rho = 1, 5, 10, 25$ to reflect four levels of spatially autocorrelated habitat. For each of the 16 scenarios (parameter sets and spatial autocorrelation), we generated 250 movement tracks $\{x_1, x_2, \ldots, x_n\}$ of length $n = 250$. For each track, we tested the inference method using 20 and 200 control locations in the Monte Carlo integration procedure (section 2.2). All parameters were estimated using MLE.

3.2 Results

In most cases, the parameters were estimated accurately, although β_2 was generally estimated more precisely than β_1 (Figure 3). The median (min, max) difference between estimated and known parameter values was -0.04 (-65, 27) for β_1 and 0.04 (-4.8, 4.7) for β_2. Spatial autocorrelation in G had a noticeable effect on the precision of β_1 estimates, but not β_2. When β_1 was high, there was a pattern of decreased precision with increased autocorrelation. When β_1 was low, precision was lowest when spatial autocorrelation was very low ($\rho = 1$) and very high ($\rho = 50$). Spatial autocorrelation is a documented issue in resource selection analyses, which can lead to biased parameter estimates (Northrup *et al.*, 2013). In SSFs and ESFs, high spatial autocorrelation decreases the range of the covariate space that may be explored for each movement step, which may decrease the ability to infer selection, particularly when the number of control locations is low (Northrup *et al.*, 2013). However, in our simulations, the number of control locations used in Monte Carlo integration had negligible effects on the precision or accuracy of parameter estimations. Therefore, in most cases, 20 control locations should be adequate to approximate the likelihood, but this also depends on the

size of the sampling radius. We still recommend caution when working with highly spatially autocorrelated environmental covariates.

4 Case Study

Polar bears are sea ice-obligate apex carnivores that forage on fat-rich prey, such as ringed seals (*Pusa hispida*) and bearded seals (*Erignathus barbatus*) (Pilfold *et al.*, 2012). Polar bear abundance, distribution, and body condition are associated with the spatial and temporal distribution of their prey (Stirling & McEwan, 1975; Pilfold *et al.*, 2014; Galicia *et al.*, 2020), as well as the sea ice habitat configuration (Rode *et al.*, 2010; Lunn *et al.*, 2016; McCall *et al.*, 2016). Energy gain is highest in the spring when bears enter a hyperphagic period (Pilfold *et al.*, 2012), before fasting for several months (Stirling & Øritsland, 1995). Therefore, polar bears have limited time to store enough energy to survive and reproduce (Stirling & Øritsland, 1995), and must balance the high-energy returns of their prey against energetic costs. Polar bears have energetically expensive locomotion (Hurst *et al.*, 1982a; Pagano *et al.*, 2018) that is affected by habitat dynamics, including sea ice drift (Durner *et al.*, 2017; Klappstein *et al.*, 2020) and fragmentation (Blanchet *et al.*, 2020). To reach or remain in preferred habitat, polar bears may oppose the moving sea ice and expend more energy to cover the same geographic distance (Mauritzen *et al.*, 2003; Auger-Méthé *et al.*, 2016; Durner *et al.*, 2017). Further, when sea ice cover is low, polar bears are more likely to swim (Pilfold *et al.*, 2016; Lone *et al.*, 2018), which is 5x more energetically expensive than walking (Griffen, 2018). These spatiotemporal interactions suggest that energetic considerations may be important in governing polar bear movement and habitat selection.

The energetics of free-ranging polar bears have yet to be analyzed in a framework that considers selection of gains and costs. Movement and habitat selection studies often consider environmental conditions with energetic implications without formulating the covariates into an energetic currency (e.g., McCall *et al.*, 2016; Johnson & Derocher, 2020) and/or only including the effect of a single covariate (e.g., Durner *et al.*, 2017; Klappstein *et al.*, 2020). When energetics have been more comprehensively considered, they have been coarsely estimated (e.g., dynamic energy budgets in Molnár *et al.*, 2011) or limited to energetic costs (Blanchet *et al.*, 2020; Pagano *et al.*, 2020). In this case study, we apply the ESF to polar bears in the Beaufort Sea, which has fast ice drift speeds and variable ice concentration

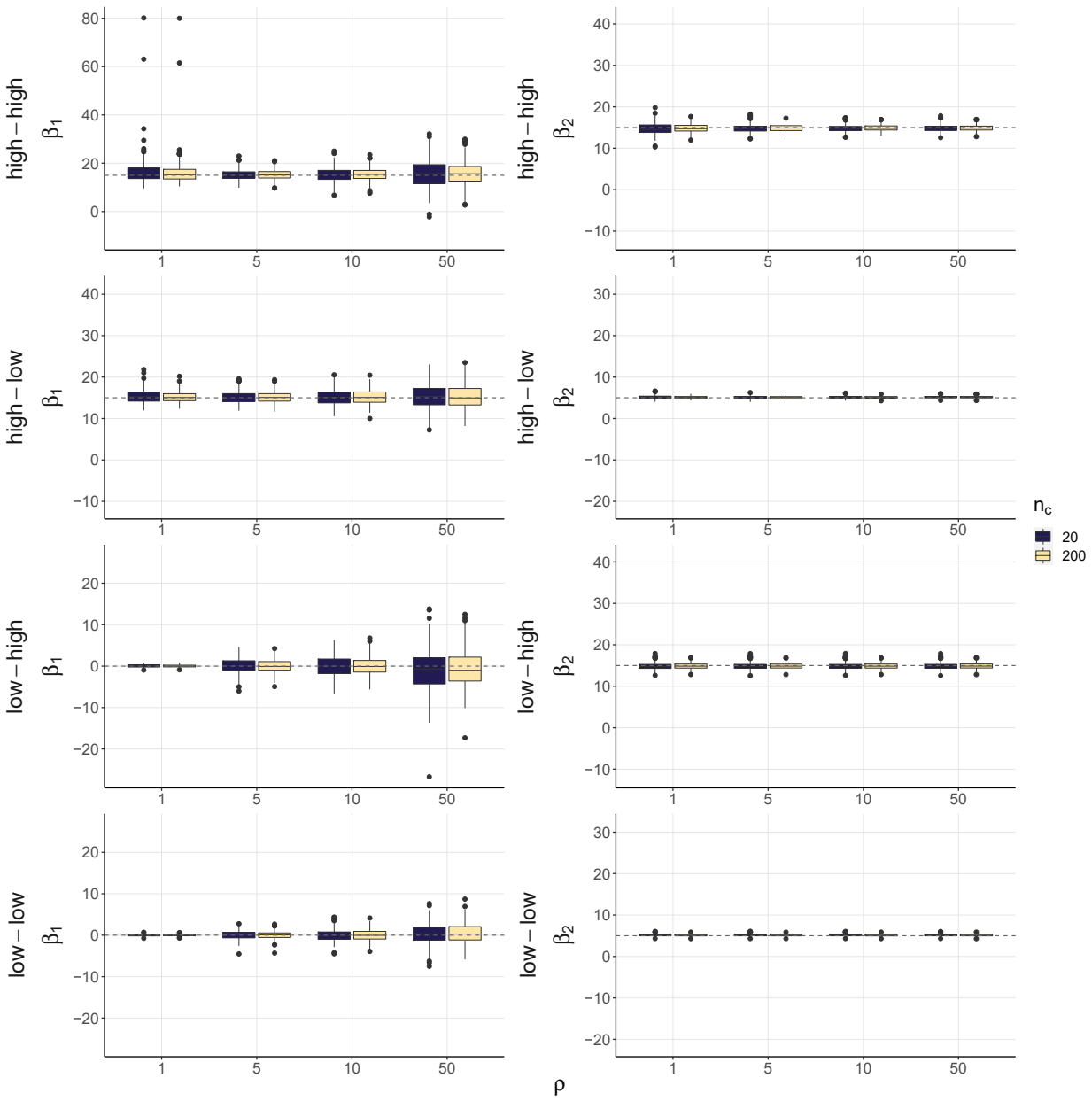

Figure 3: Parameter estimates from the simulations, under 32 different scenarios. Tracks were simulated with four sets of parameters: "high-high" ($\beta_1 = 15$, $\beta_2 = 15$), "high-low" ($\beta_1 = 15$, $\beta_2 = 5$), "low-high" ($\beta_1 = 0$, $\beta_2 = 15$), and "low-low" ($\beta_1 = 0$, $\beta_2 = 5$). ρ refers to the level of spatial autocorrelation in the energetic gain covariate G, and n_c is the number of controls used in Monte Carlo integration. Dashed line is the true parameter value.

(Carmack & Macdonald, 2002). We estimate energetic gains from an energetically-weighted RSF of seal kills, and develop a cost model for use with GPS telemetry data. Therefore, we consider polar bear energetics at the scale of movement-based habitat selection.

4.1 Methods

Data Processing

We analyzed 4-hour resolution telemetry data from 23 GPS-collared solitary adult (> 5 years old) female polar bears from 2007-2011 in the Canadian Beaufort Sea (Figures 4, A.4; Appendix 2). We calculated body mass from axillary girth and body length measurements (Thiemann *et al.*, 2011). We omitted GPS locations from dropped collars or deceased bears, following Togunov *et al.* (2020). We defined a movement burst as a sequence of locations with no gaps > 24 hours and only kept bursts with ≥ 10 locations. We calculated step length as the Euclidean distance between projected GPS locations (NAD83 UTM Zone 9N, EPSG:3156), and removed unrealistic locations where the step speed was > 5.4 km/h (Whiteman *et al.*, 2015). Then, we imputed missing locations of each burst with a continuous-time correlated random walk model (Johnson *et al.*, 2008), implemented in *momentuHMM* (McClintock & Michelot, 2018). We interpolated relevant environmental variables (described below) with bilinear interpolation (Figure 4), using the *raster* package.

Energetic Gains G

We derived energetic gains from an RSF model of forage quality from Pilfold *et al.* (2014). The RSF modelled locations of seals killed by polar bears, weighted by biomass, relative to habitat characteristics (see Pilfold *et al.*, 2014). Because the RSF incorporated both seal biomass and abundance, we assumed the raw RSF value to be proportional to energetic return. We extended both the temporal and spatial extent of the original rasters (Figure 4). We created daily rasters which encompassed approximately 100km off-shore along the coast of Alaska and Canada (from approximately 160°W to 115°W), including the Amundsen Gulf and regions adjacent to Banks Island from March-June of 2007-2011. The resolution of the rasters was 6.25km and RSF values were zero in locations where sea ice was absent.

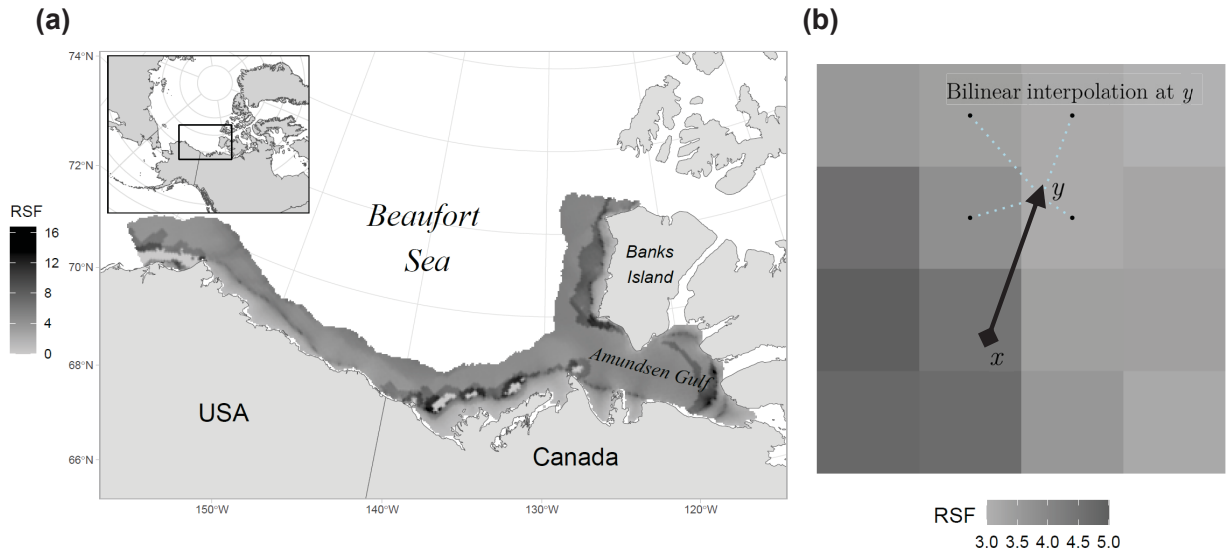

Figure 4: Illustration of energetic gains in polar bear case study. (a) Map of study area overlaid with an example seal biomass RSF (Pilfold *et al.*, 2014). (b) Schematic representation of energetic gain evaluation for a step from x to y, using bilinear interpolation at y based on the four adjacent cells (black dots).

Energetic Costs C

We formulated costs based on the movement costs of captive polar bears, combined with environmental covariates to better represent field conditions (Figure 5). Telemetry locations arise from a combination of active bear movement and passive displacement caused by ice drift (Mauritzen *et al.*, 2003; Auger-Méthé *et al.*, 2016; Durner *et al.*, 2017). Therefore, we define a step as the active bear movement between telemetry locations, corrected for ice drift following Klappstein *et al.* (2020), using drift data from the National Snow and Ice Data Center (Polar Pathfinder Daily 25km EASE-Grid Sea Ice Motion Vectors; Tschudi *et al.*, 2019). At each step, a bear can either be swimming or walking on sea ice, which have distinct energetic costs (e.g., Hurst *et al.*, 1982a; Griffen, 2018; Pagano *et al.*, 2018). Using aquatic sensor data from Lone *et al.* (2018), we modelled the relationship between the proportion of time in water and sea ice concentration as a generalized additive model (GAM) in the *mgcv* package (Wood, 2017). Using this curve, we estimated proportion of time spent in water for each polar bear step, which we assumed to be the same as the proportion of the distance travelled. Lastly, we modelled the relationship between travel speed and energy expenditure,

using combined estimates from five treadmill studies (Øritsland & Jonker, 1976; Hurst *et al.*, 1982a,b; Watts *et al.*, 1991; Pagano *et al.*, 2018). We modelled energy expenditure as a function of walking speed as a GAM with a gamma response distribution and a positive monotonic constraint in the R package *scam* (Pya & Wood, 2015; Pya, 2019). When the bear was assumed to be walking, the cost was derived directly from this curve, and when the bear was swimming, we multiplied this cost by five to represent the higher energy expenditure (Griffen, 2018). Our modelling approach estimated similar daily costs as those obtained from doubly-labelled water (Figure A.5).

Fitting the ESF

We eliminated locations that were outside the spatiotemporal extent of prey data availability (Figures 5, A.4). We generated 20 control locations on a disc around each observed location, with radius $R = 1.1 \times l_m$, where l_m is the maximum step length of all observed locations (see Appendix 1 for justification of R). We calculated energetic gains and costs of each step as described above, using environmental covariate values at each end location. We omitted steps from analysis when there was > 10 control locations without an energetic gain estimate (i.e., outside the raster extent). We fit the ESF with the numerical optimizer *optim* separately for each bear. We calculated confidence intervals (CIs) based on the approximate standard errors of the maximum likelihood estimates, obtained from the inverse of the Hessian matrix given by *optim*. Lastly, in Appendix 2.3, we compare the ESF to a null model. We write a simple random walk (SRW) model as a special case of the ESF, where there is no effect of energetic gains and costs are defined as l^2. By using the same implementation procedure, we can therefore assess support for the ESF against this simpler movement model using Akaike's Information Criterion (AIC).

4.2 Results

We analyzed $7,861$ GPS locations (locations per individual: $80 - 968$). Energetic gains at each step (including controls) ranged from 0 to 27.9 (unitless) and energetic costs ranged from 3.27 to 161 MJ. The median β_1 estimate was -0.01 (range $-0.29, 0.83$), but only four estimates had CIs that did not overlap zero (Figure 6). Only three bears selected for energetic gains ($\beta_1 \pm 95\%$ CI $= 0.83 \pm 0.82$; 0.32 ± 0.20; 0.28 ± 0.17) and one bear selection against energetic gains ($\beta_1 \pm 95\%$ CI $= -0.29 \pm 0.20$). All β_2 estimates showed a selection against

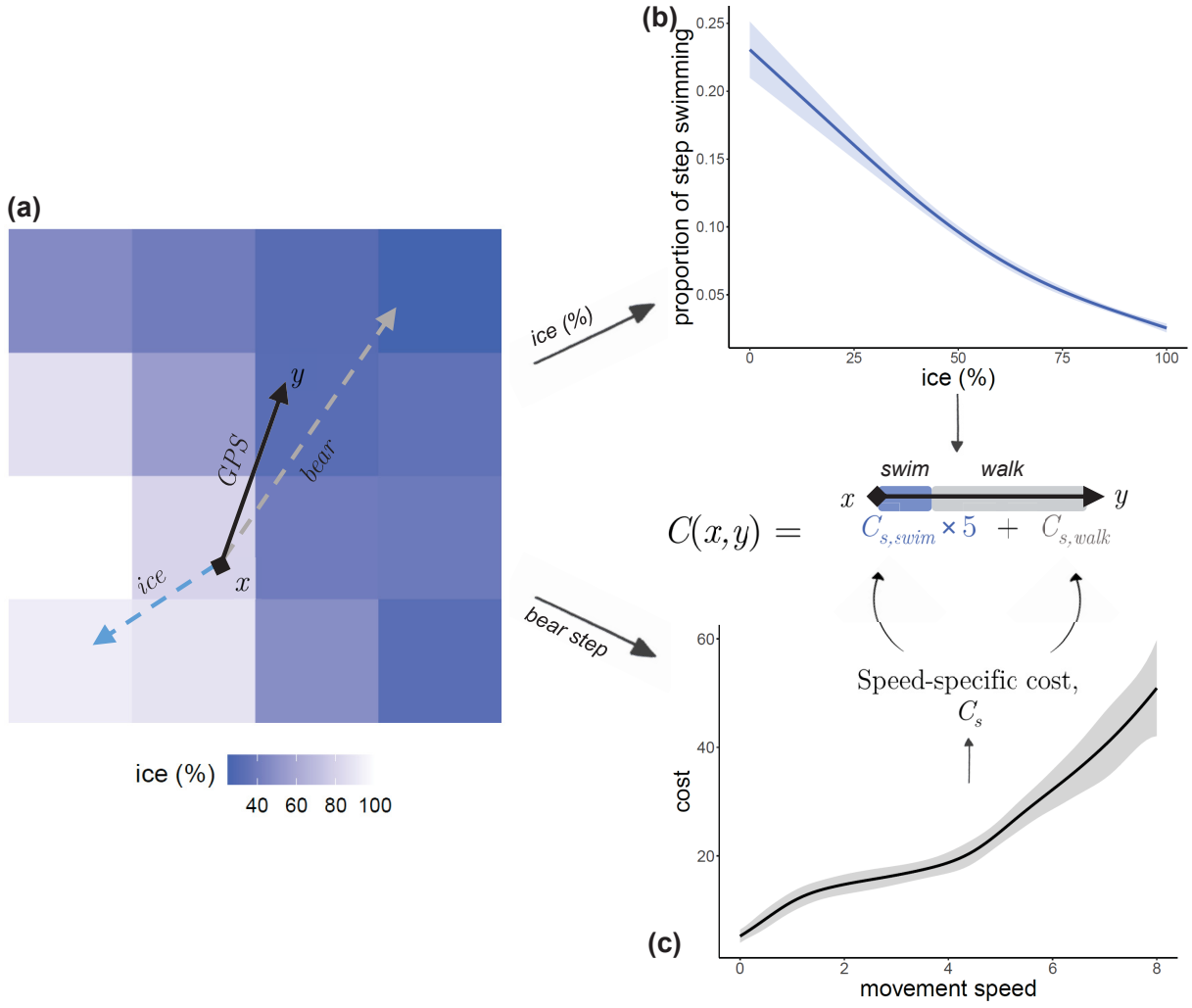

Figure 5: Schematic illustration of energetic cost evaluation in the polar bear case study, for an observed step starting at x and ending at y. (a) Arrows represent the observed movement step (black; GPS), ice drift (blue dashed; ice), and actual bear movement (grey dashed; calculated as GPS - ice). Ice concentration (%) is estimated at y with bilinear interpolation. (b) Modelled relationship between ice concentration and the proportion of the step spent swimming from Lone *et al.* (2018). We use the estimated ice % from (a) to estimate the proportion of the bear step spent swimming and walking. (c) Modelled relationship between polar bear movement speed (km/h) and energetic cost (kJ/kg/h) from several treadmill studies. Using the bear speed and weight, we calculate C_s for the step. $C_{s,swim}$ and $C_{s,walk}$ are C_s multiplied by the proportion of time in each behaviour. The total energy expenditure of the step $C(x, y)$ is the sum of $C_{s,swim}$ multiplied by 5 (to represent the higher costs of swimming) and $C_{s,walk}$.

costs, with a median of 0.57 (range $0.32, 0.97$), and no CIs overlapped zero. The ESF fit better than the null model (SRW) in all but three cases, indicating that polar bears follow a cost-minimization pattern, rather than simple Brownian motion (Appendix 2.3).

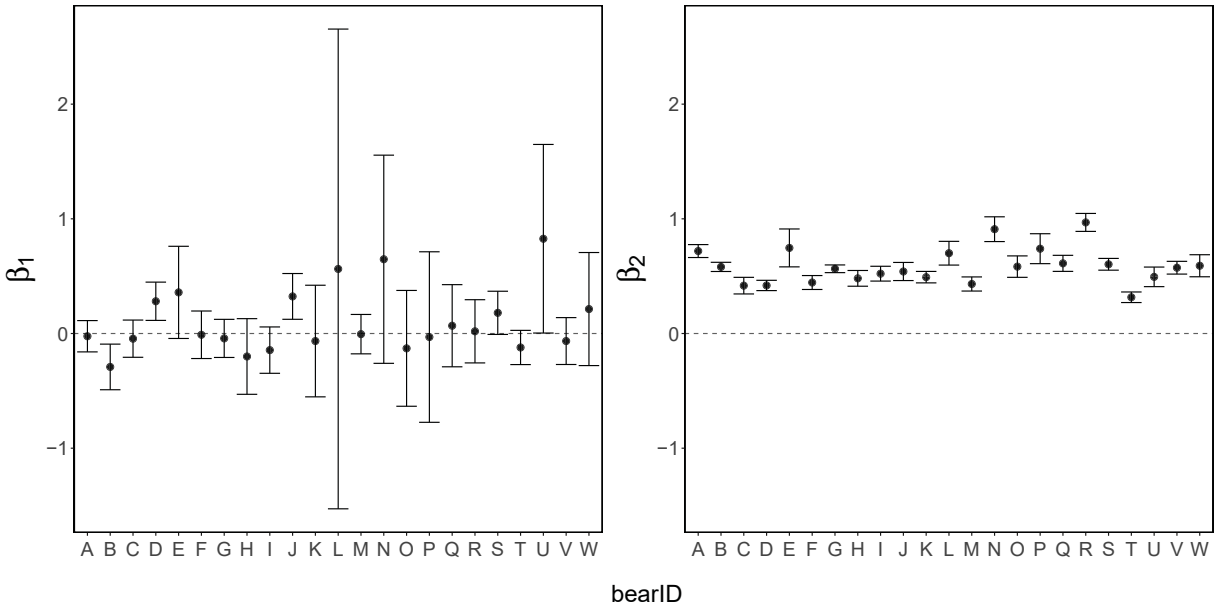

Figure 6: Estimated β_1 (selection for gains) and β_2 (selection against costs) coefficients of lone adult female polar bears ($N = 23$). Error bars are 95% CIs and dashed line is at 0.

4.3 Discussion

In this case study, we found a strong pattern of selection against energetic costs in all individuals, but only four showed selection for ($n = 3$) or against ($n = 1$) energetic gains. However, effects may have been hard to detect if the grain size and spatial autocorrelation of our covariate data were too high for the temporal scale and spatial domain size of the telemetry data (Boyce *et al.*, 2003; Boyce, 2006; Northrup *et al.*, 2013). This could result in low variation between case and control locations, particularly if the tracking data is not at a biologically relevant resolution. Future studies should assess the effect of scale on polar bear energy selection. Further, our uncertainty estimates do not consider the error in our covariate data (Pilfold *et al.*, 2014; Tschudi *et al.*, 2019; Togunov *et al.*, 2020), which may affect modelling outcomes (Van Niel & Austin, 2007). However, error propagation is not standard in habitat selection studies, as methods remain analytically complex and

uncertainty in environmental data is often unknown (Molto *et al.*, 2013). Lastly, we did not incorporate movement speed into G nor turning angle into C, due to lack of empirical data to support their inclusion.

Despite the above caveats, our results suggest that most solitary female polar bears in the Beaufort Sea employ a cost-minimization strategy. Cost-minimization could arise due to high predictability of energy expenditure, based on internal factors and mechanical movement constraints, while energy-maximization would require polar bears to have knowledge of the unpredictable seal distribution (Ramsay & Stirling, 1986; Ferguson *et al.*, 1999). At the landscape level, polar bear distribution correlates positively to seal biomass (Pilfold *et al.*, 2014), but we did not observe this at the scale of the movement step, which may be reflective of local variability in seal distribution. Further, our model assumes that energy selection is consistent through time and across behaviours, although selection for gains is likely variable over the study period. Polar bears do not enter the main foraging period until mid-April (Pilfold *et al.*, 2012) and continue to gain weight into the summer months (Galicia *et al.*, 2020). From March to May, solitary females may also pair with males for mating, during which they forage less frequently and are sequestered from ideal habitats for up to 18 days at a time (Wiig *et al.*, 1992; Derocher *et al.*, 2010; Stirling *et al.*, 2016). Additionally, polar bear movements may be influenced by site fidelity (Mauritzen *et al.*, 2001), in which recurrent space-use patterns dominate short-term selection for energetic gains. If selection for gains is affected by competing behaviours, it may be that only individuals with exceptionally strong selection may be identified. These hypotheses should be tested in future research, which may require a more nuanced model formulation, while addressing annual, seasonal, demographic, and spatial variation in energy selection.

5 Discussion and Conclusions

Evaluating the energetic basis of animal movement and habitat selection remains a topical issue in ecology (Eisaguirre *et al.*, 2020; Pagano *et al.*, 2020; Williams *et al.*, 2020). Our new model to estimate the energy preferences of animals is similar to recent approaches to combine movement and habitat (Avgar *et al.*, 2016; Michelot *et al.*, 2019), but the ESF uniquely integrates both factors into energetic covariates. Therefore, our approach explicitly accounts for energetics in the selection process, unlike similar work by Eisaguirre *et al.* (2020),

which incorporated costs into the availability kernel. We applied the ESF to lone female polar bears and found that cost-minimization the most common energetic strategy, which helps explain their movement in dynamic habitats. We consider this model an important step towards more realistic models to uncover the contribution of energy in observed space use patterns.

The performance of the ESF depends on our ability to accurately define the energetic covariates, which relies on evaluating complex interactions between movement and habitat. Mischaracterization of the covariates may lead to biased estimates that do not truly represent energy selection. Challenges in evaluating G and C will be case-specific, but would most likely arise from insufficient empirical data. In particular, it may not be possible to include all relevant energetic factors (e.g., every resource that an animal may forage on or the exact effect of movement or habitat composition on the covariates). In many studies, it may also be impossible to express G and C in the same unit, or to account for energy assimilation and conversion rates, which would facilitate comparison of β_1 and β_2 (i.e., relative strength of selection). However, even when the covariates are expressed in different units, we can still make comparisons between individuals or other temporal or demographic factors, as illustrated in Section 4. Further, it is important that the spatial scale of the covariate data be complementary to the temporal resolution of the tracking data, and that the tracking data is at the scale at which energy selection is expected to occur. We hope that this study will motivate the collection of more precise data to better understand the energetic mechanisms behind animal movements.

The ESF has close theoretical and practical links to existing methods (SSFs and iSSA), with great potential for methodological extensions. We could add separate terms to the model, such as movement metrics (similar to iSSA; Avgar *et al.*, 2016) or terms with no energetic interpretation. This may prove useful to account for movement when it cannot be included in G and C and to assess energetic trade-offs. Another possible extension would be to consider a state-switching ESF model, where an unobserved behavioural state determines the selection parameters for energetic gains and costs. This could be written as a hidden Markov model, similarly to the state-switching SSF model of Nicosia *et al.* (2017). Ultimately, the ESF is a flexible method to combine energy, movement, and habitat selection, and is applicable to any study species or system with adequate data.

References

Arthur, S. M., Manly, B. F. J., Mcdonald, L. L. & Garner, G. W. (1996). Assessing Habitat Selection when Availability Changes. *Ecology*, 77, 215–227.

Auger-Méthé, M., Lewis, M. A. & Derocher, A. E. (2016). Home ranges in moving habitats: Polar bears and sea ice. *Ecography*, 39, 26–35.

Avgar, T., Potts, J. R., Lewis, M. A. & Boyce, M. S. (2016). Integrated step selection analysis: bridging the gap between resource selection and animal movement. *Methods in Ecology and Evolution*, 7, 619–630.

Bartumeus, F. & Catalan, J. (2009). Optimal search behavior and classic foraging theory. *Journal of Physics A: Mathematical and Theoretical*, 42, 434002.

Bastille-Rousseau, G., Wall, J., Douglas-Hamilton, I., Lesowapir, B., Loloju, B., Mwangi, N. & Wittemyer, G. (2020). Landscape-scale habitat response of African elephants shows strong selection for foraging opportunities in a human dominated ecosystem. *Ecography*, 43, 149–160.

Bidder, O. R., Goulding, C., Toledo, A., Van Walsum, T. A., Siebert, U. & Halsey, L. G. (2017). Does the Treadmill Support Valid Energetics Estimates of Field Locomotion? *Integrative and Comparative Biology*, 57, 301–319.

Blanchet, M., Aars, J., Andersen, M. & Routti, H. (2020). Space-use strategy affects energy requirements in Barents Sea polar bears. *Marine Ecology Progress Series*, 639, 1–19.

Bonnell, T. R., Campennì, M., Chapman, C. A., Gogarten, J. F., Reyna-Hurtado, R. A., Teichroeb, J. A., Wasserman, M. D. & Sengupta, R. (2013). Emergent Group Level Navigation: An Agent-Based Evaluation of Movement Patterns in a Folivorous Primate. *PLoS ONE*, 8, e78264.

Boyce, M. S. (2006). Scale for resource selection functions. *Diversity and Distributions*, 12, 269–276.

Boyce, M. S., Mao, J. S., Merrill, E. H., Fortin, D., Turner, M. G., Fryxell, J. & Turchin, P. (2003). Scale and heterogeneity in habitat selection by elk in Yellowstone National Park. *Ecoscience*, 10, 421–431.

Burnham, K. P. & Anderson, D. R. (2002). *Model Selection and Multimodel Inference: A Practical Information-Theoretic Approach*. 2nd edn. Springer-Verlag, New York. ISBN 0387953647.

Butler, P. J., Green, J. A., Boyd, I. L. & Speakman, J. R. (2004). Measuring metabolic rate in the field: the pros and cons of the doubly labelled water and heart rate methods. *Functional Ecology*, 18, 168–183.

Calvert, W. & Ramsay, M. A. (1998). Evaluation of Age Determination of Polar Bears by Counts of Cementum Growth Layer Groups. *Ursus*, 10, 449–453.

Carmack, E. C. & Macdonald, R. W. (2002). Oceanography of the Canadian shelf of the Beaufort Sea: A setting for marine life. *Arctic*, 55, 29–45.

Chapman, J. W., Klaassen, R. H. G., Drake, V. A., Fossette, S., Hays, G. C., Metcalfe, J. D., Reynolds, A. M., Reynolds, D. R. & Alerstam, T. (2011). Animal orientation strategies for movement in flows. *Current Biology*, 21, R861–R870.

Charnov, E. L. (1976). Optimal foraging: The marginal value theorem. *Theoretical Population Biology*, 9, 129–136.

Codling, E. A., Plank, M. J. & Benhamou, S. (2008). Random walk models in biology. *Journal of the Royal Society Interface*, 5, 813–834.

Crête, M. & Larivière, S. (2003). Estimating the costs of locomotion in snow for coyotes. *Canadian Journal of Zoology*, 81, 1808–1814.

Derocher, A. E., Andersen, M., Wiig, Ø. & Aars, J. (2010). Sexual dimorphism and the mating ecology of polar bears (Ursus maritimus) at Svalbard. *Behavioral Ecology and Sociobiology*, 64, 939–946.

Durner, G. M., Douglas, D. C., Albeke, S. E., Whiteman, J. P., Amstrup, S. C., Richardson, E. S., Wilson, R. R. & Ben-David, M. (2017). Increased Arctic sea ice drift alters adult female polar bear movements and energetics. *Global Change Biology*, 23, 3460–3473.

Eisaguirre, J. M., Booms, T. L., Barger, C. P., Lewis, S. B. & Breed, G. A. (2020). Novel step selection analyses on energy landscapes reveal how linear features alter migrations of soaring birds. *Journal of Animal Ecology*, 89, 2567–2583.

Emlen, J. M. (1966). The Role of Time and Energy in Food Preference. *The American Naturalist*, 100, 611–617.

Ferguson, S. H., Taylor, M. K., Born, E. W., Rosing-Asvid, A. & Messier, F. (1999). Determinants of home range size for polar bears (Ursus maritimus). *Ecology Letters*, 2, 311–318.

Forester, J., Kyung Im, H. & Rathouz, P. (2009). Accounting for animal movement in estimation of resource selection functions: sampling and data analysis. *Ecology*, 90, 3554–3565.

Fortin, D., Beyer, H. L., Boyce, M. S., Smith, D. W., Duchesne, T. & Mao, J. S. (2005). Wolves influence elk movements: behaviour shapes a trophic cascade in Yellowstone National Park. *Ecology*, 86, 1320–1330.

Fortin, D., Fryxell, J. M., O'brodovich, L. & Frandsen, D. (2003). Foraging ecology of bison at the landscape and plant community levels: the applicability of energy maximization principles. *Oecologia*, 134, 219–227.

Galicia, M. P., Thiemann, G. W. & Dyck, M. G. (2020). Correlates of seasonal change in the body condition of an Arctic top predator. *Global Change Biology*, 26, 840–850.

Gallagher, A. J., Creel, S., Wilson, R. P. & Cooke, S. J. (2017). Energy Landscapes and the Landscape of Fear. *Trends in Ecology & Evolution*, 32, 88–96.

Griffen, B. D. (2018). Modeling the metabolic costs of swimming in polar bears (Ursus maritimus). *Polar Biology*, 41, 491–503.

Halsey, L. G. (2016). Terrestrial movement energetics: current knowledge and its application to the optimising animal. *Journal of Experimental Biology*, 219, 1424–1431.

Halsey, L. G. (2017). Relationships grow with time: a note of caution about energy expenditure-proxy correlations, focussing on accelerometry as an example. *Functional Ecology*, 31, 1176–1183.

Hansen, B. B., Herfindal, I., Aanes, R., Sæther, B. E. & Henriksen, S. (2009). Functional response in habitat selection and the tradeoffs between foraging niche components in a large herbivore. *Oikos*, 118, 859–872.

Higginson, A. D. & Ruxton, G. D. (2015). Foraging mode switching: The importance of prey distribution and foraging currency. *Animal Behaviour*, 105, 121–137.

Hurst, R. J., Leonard, M. L., Watts, P. D., Beckerton, P. & Øritsland, N. a. (1982a). Polar bear locomotion: body temperature and energetic cost. *Canadian Journal of Zoology*, 60, 40–44.

Hurst, R. J., Øritsland, N. & Watts, P. (1982b). Body mass, temperature and cost of walking in polar bears. *Acta Physiologica Scandinavica*, 115, 391–395.

Hutchings, J. K. & Rigor, I. G. (2012). Role of ice dynamics in anomalous ice conditions in the Beaufort Sea during. *Journal of Geophysical Research*, 117, C00E04.

Johnson, A. C. & Derocher, A. E. (2020). Variation in habitat use of Beaufort Sea polar bears. *Polar Biology*, 43, 1247–1260.

Johnson, D. S., London, J. M., Lea, M.-A. & Durban, J. W. (2008). Continous-time correlated random walk model for animal telemetry data. *Ecology*, 89, 1208–1215.

Klappstein, N. J., Togunov, R. R., Reimer, J. R., Lunn, N. J. & Derocher, A. E. (2020). Patterns of sea ice drift and polar bear (Ursus maritimus) movement in Hudson Bay. *Marine Ecology Progress Series*, 641, 227–240.

Lone, K., Kovacs, K. M., Lydersen, C., Fedak, M., Andersen, M., Lovell, P. & Aars, J. (2018). Aquatic behaviour of polar bears (Ursus maritimus) in an increasingly ice-free Arctic. *Scientific Reports*, 8, 9677.

Lunn, N. J., Servanty, S., Regehr, E. V., Converse, S. J., Richardson, E. S. & Stirling, I. (2016). Demography of an apex predator at the edge of its range: impacts of changing sea ice on polar bears in Hudson Bay. *Ecological Applications*, 26, 1302–1320.

MacArthur, R. H. & Pianka, E. R. (1966). On Optimal Use of a Patchy Environment. *The American Naturalist*, 100, 603–609.

Manly, B. F., McDonald, L. L., Thomas, D. L., McDonald, T. L. & Erickson, W. P. (2002). *Resource selection by animals:statistical design and analysis for field studies*, vol. 34. 2nd edn. Kluwer Academic Publishers, Dordecht. ISBN 0306481510.

Mauritzen, M., Derocher, A. E., Pavlova, O. & Wiig, Ø. (2003). Female polar bears, Ursus maritimus, on the Barents Sea drift ice: walking the treadmill. *Animal Behaviour*, 66, 107–113.

Mauritzen, M., Derocher, A. E. & Wiig, Ø. (2001). Space-use strategies of female polar bears in a dynamic sea ice habitat. *Canadian Journal of Zoology*, 79, 1704–1713.

McCall, A. G., Pilfold, N. W., Derocher, A. E. & Lunn, N. J. (2016). Seasonal habitat selection by adult female polar bears in western Hudson Bay. *Population Ecology*, 58, 407–419.

McClintock, B. T. & Michelot, T. (2018). momentuHMM: R package for generalized hidden Markov models of animal movement. *Methods in Ecology and Evolution*, 9, 1518–1530.

McNarry, M. A., Wilson, R. P., Holton, M. D., Griffiths, I. W. & Mackintosh, K. A. (2017). Investigating the relationship between energy expenditure, walking speed and angle of turning in humans. *PLoS ONE*, 12, e0182333.

Michelot, T. (2019). *Stochastic models of animal movement and habitat selection*. Ph.D. thesis, University of Sheffield.

Michelot, T., Blackwell, P. G. & Matthiopoulos, J. (2019). Linking resource selection and step selection models for habitat preferences in animals. *Ecology*, 100, e02452.

Molnár, P. K., Derocher, A. E., Klanjscek, T. & Lewis, M. A. (2011). Predicting climate change impacts on polar bear litter size. *Nature Communications*, 2, 186.

Molto, Q., Rossi, V. & Blanc, L. (2013). Error propagation in biomass estimation in tropical forests. *Methods in Ecology and Evolution*, 4, 175–183.

Nagy, K. A. (1989). Field Bioenergetics: Accuracy of Models and Methods. *Physiological Zoology*, 62, 237–252.

Nathan, R., Getz, W. M., Revilla, E., Holyoak, M., Kadmon, R., Saltz, D. & Smouse, P. E. (2008). A movement ecology paradigm for unifying organismal movement research. *Proceedings of the National Academy of Sciences*, 105, 19052–19059.

Nicosia, A., Duchesne, T., Rivest, L.-P. & Fortin, D. (2017). A multi-state conditional logistic regression model for the analysis of animal movement. *The Annals of Applied Statistics*, 11, 1537–1560.

Northrup, J. M., Hooten, M. B., Anderson, C. R. J. & Wittemyer, G. (2013). Practical guidance on characterizing availability in resource selection functions under a use-availability design. *Ecology*, 94, 1456–1463.

Øritsland, N. & Jonker, W. (1976). A respiration chamber for exercising polar bears. *Norwegian Journal of Zoology*, 24, 65–67.

Owen-Smith, N., Fryxell, J. M. & Merrill, E. H. (2010). Foraging theory upscaled: the behavioural ecology of herbivore movement. *Philosophical Transactions of the Royal Society Series B: Biological Sciences*, 365, 2267–2278.

Pagano, A. M., Atwood, T. C., Durner, G. M. & Williams, T. M. (2020). The seasonal energetic landscape of an apex marine carnivore, the polar bear. *Ecology*, 101, 1–16.

Pagano, A. M., Durner, G. M., Rode, K. D., Atwood, T. C., Atkinson, S. N., Peacock, E., Costa, D. P., Owen, M. A. & Williams, T. M. (2018). High-energy, high-fat lifestyle challenges an Arctic apex predator, the polar bear. *Science*, 359, 568–572.

Pagano, A. M. & Williams, T. M. (2019). Estimating the energy expenditure of free-ranging polar bears using tri-axial accelerometers: A validation with doubly labeled water. *Ecology and Evolution*, 9, 4210–4219.

Petty, A. A., Hutchings, J. K., Richter-Menge, J. A. & Tschudi, M. A. (2016). Sea ice circulation around the Beaufort Gyre: The changing role of wind forcing and the sea ice state. *Journal of Geophysical Research: Oceans*, 121, 3278–3296.

Pilfold, N. W., Derocher, A. E. & Richardson, E. S. (2014). Influence of intraspecific competition on the distribution of a wide-ranging, non-territorial carnivore. *Global Ecology and Biogeography*, 23, 425–435.

Pilfold, N. W., Derocher, A. E., Stirling, I., Richardson, E. S. & Andriashek, D. S. (2012). Age and Sex Composition of Seals Killed by Polar Bears in the Eastern Beaufort Sea. *PLoS ONE*, 7, e41429.

Pilfold, N. W., Hedman, D., Stirling, I., Derocher, A. E., Lunn, N. J. & Richardson, E. S. (2016). Mass Loss Rates of Fasting Polar Bears. *Physiological and Biochemical Zoology*, 89, 377–388.

Potts, J. R., Bastille-Rousseau, G., Murray, D. L., Schaefer, J. A. & Lewis, M. A. (2014). Predicting local and non-local effects of resources on animal space use using a mechanistic step selection model. *Methods in Ecology and Evolution*, 5, 253–262.

Pya, N. (2019). scam: Shape Constrained Additive Models. R package version 1.2-5. URL `https://cran.r-project.org/package=scam`.

Pya, N. & Wood, S. N. (2015). Shape constrained additive models. *Statistics and Computing*, 25, 543–559.

Pyke, G. H. (2015). Understanding movements of organisms: it's time to abandon the Lévy foraging hypothesis. *Methods in Ecology and Evolution*, 6, 1–16.

Pyke, G. H. (2019). Animal movements - an optimal foraging theory approach. In: *Encyclopedia of Animal Behavior*, vol. 2, 2nd edn. Elsevier. ISBN 9780128132517, pp. 149–156.

Pyke, G. H., Pulliam, H. R. & Charnov, E. L. (1977). Optimal foraging: A selective review of theory and tests. *The Quarterly Review of Biology*, 52, 137–154.

Ramsay, M. A. & Stirling, I. (1986). On the mating system of polar bears. *Canadian Journal of Zoology*, 64, 2142–2151.

Reynolds, A. (2013). Beyond Optimal Searching: Recent Developments in the Modelling of Animal Movement Patterns as Lévy Walks. In: *Dispersal, Individual Movement and Spatial Ecology. Lecture Notes in Mathematics, vol 2071.* (eds. Lewis, M. A., Maini, P. K. & Petrovskii, S. V.). Springer, Berlin, Heidelberg, pp. 53–79.

Rhodes, J. R., Mcalpine, C. A., Lunney, D. & Possingham, H. P. (2005). A spatially explicit habitat selection model incorporating home range behavior. *Ecology*, 86, 1199–1205.

Rode, K. D., Amstrup, S. C. & Regehr, E. V. (2010). Reduced body size and cub recruitment in polar bears associated with sea ice decline. *Ecological Applications*, 20, 768–782.

Schoener, T. W. (1971). Theory of Feeding Strategies. *Annual Review of Ecology and Systematics*, 2, 369–404.

Shepard, E. L. C., Wilson, R. P., Quintana, F., Gó Mez Laich, A. & Forman, D. W. (2009). Pushed for time or saving on fuel: fine-scale energy budgets shed light on currencies in a diving bird. *Proceedings of the Royal Society B*, 276, 3149–3155.

Shepard, E. L. C., Wilson, R. P., Rees, W. G., Grundy, E., Lambertucci, S. A. & Vosper, S. B. (2013). Energy landscapes shape animal movement ecology. *The American Naturalist*, 182, 298–312.

Shlesinger, M. & Klafter, J. (1986). Lévy Walks Versus Lévy Flights. In: *On Growth and Form. NATO ASI Series (Series E: Applied Sciences)* (eds. Stanley, H. & Ostrowsky, N.). Springer, Dordrecht, pp. 279–283.

Sih, A. (1984). Optimal Behavior and Density-Dependent Predation. *The American Naturalist*, 123, 314–326.

Speakman, J. (1997). *Doubly labelled water: theory and practice*. 1st edn. Chapman & Hill, London.

Stern, H. L. & Laidre, K. L. (2016). Sea-ice indicators of polar bear habitat. *Cryosphere*, 10, 2027–2041.

Stirling, I. & McEwan, E. H. (1975). The caloric value of whole ringed seals (Phoca hispida) in relation to polar bear (Ursus maritimus) ecology and hunting behavior. *Canadian Journal of Zoology*, 53, 1021–1027.

Stirling, I. & Øritsland, N. (1995). Relationships between estimates of ringed seal (Phoca hispida) and polar bear (Ursus maritimus) populations in the Canadian Arctic. *Canadian Journal of Fisheries and Aquatic Sciences*, 52, 2594–2612.

Stirling, I., Spencer, C. & Andriashek, D. (2016). Behavior and activity budgets of wild breeding polar bears (Ursus maritimus). *Marine Mammal Science*, 32, 13–37.

Stirling, I., Spencer, C. & Andriashek, D. S. (1989). Immobilization of polar bears (Ursus maritimus) with Telazol in the Canadian Arctic. *Journal of Wildlife Diseases*, 25, 159–168.

Taylor, C. R., Schmidt-Nielsen, K. & Raab, J. L. (1970). Scaling of energetic cost of running to body size in mammals. *The American Journal of Physiology*, 219, 1104–1107.

Thiemann, G. W., Sciences, B. & Tg, C. A. B. (2011). Temporal Change in the Morphometry – Body Mass Relationship of Polar Bears. *Journal of Wildlife Management*, 75, 580–587.

Thurfjell, H., Ciuti, S. & Boyce, M. S. (2014). Applications of step-selection functions in ecology and conservation. *Movement Ecology*, 4, 1–12.

Togunov, R. R., Klappstein, N. J., Lunn, N. J., Derocher, A. E. & Auger-Méthé, M. (2020). Opportunistic evaluation of modelled sea ice drift using passively drifting telemetry collars in Hudson Bay, Canada. *The Cryosphere*, 14, 1937–1950.

Tschudi, M., Meier, W. N., Stewart, J. S., Fowler, C. & Maslanik, J. (2019). Polar Pathfinder Weekly 25 km EASE-Grid Sea Ice Motion Vectors, Version 4, Northern Hemisphere. URL `https://doi.org/10.5067/INAWUWO7QH7B`.

Van Der Post, D. J. & Semmann, D. (2011). Local Orientation and the Evolution of Foraging: Changes in Decision Making Can Eliminate Evolutionary Trade-offs. *PLoS Computational Biology*, 7, e1002186.

Van Niel, K. P. & Austin, M. P. (2007). Predictive vegetation modeling for conservation: Impact of error propagation from digital elevation data. *Ecological Applications*, 17, 266–280.

Viswanathan, G. M., Buldyrev, S. V., Havlin, S., da Luzk, M. G. E., Raposok, E. P. & Stanley, H. E. (1999). Optimizing the success of random searches. *Nature*, 401, 911–914.

Watts, P. D., Ferguson, K. L. & Draper, B. A. (1991). Energetic output of subadult polar bears (Ursus maritimus): Resting, disturbance and locomotion. *Comparative Biochemistry and Physiology*, 98A, 191–193.

Whiteman, J. P., Harlow, H. J., Durner, G. M., Anderson-Sprecher, R., Albeke, S. E., Regehr, E. V., Amstrup, S. C. & Ben-David, M. (2015). Summer declines in activity and body temperature offer polar bears limited energy savings. *Science*, 349, 295–298.

Wiig, Ø., Gjertz, I., Hansson, R. & Thomassen, J. (1992). Breeding behaviour of polar bears in Hornsund, Svalbard. *Polar Record*, 28, 157–159.

Williams, T. M., Peter-Heide Jørgensen, M., Pagano, A. M. & Bryce, C. M. (2020). Hunters versus hunted: New perspectives on the energetic costs of survival at the top of the food chain. *Functional Ecology*, 34, 2015–2029.

Wilson, R. P., Börger, L., Holton, M. D., Scantlebury, D. M., Gómez-Laich, A., Quintana, F., Rosell, F., Graf, P. M., Williams, H., Gunner, R., Hopkins, L., Marks, N., Geraldi, N. R., Duarte, C. M., Scott, R., Strano, M. S., Robotka, H., Eizaguirre, C., Fahlman, A. & Shepard, E. L. (2020). Estimates for energy expenditure in free-living animals using acceleration proxies: A reappraisal. *Journal of Animal Ecology*, 89, 161–172.

Wilson, R. P., Griffiths, I. W., Legg, P. A., Friswell, M. I., Bidder, O. R., Halsey, L. G., Lambertucci, S. A. & Shepard, E. L. C. (2013). Turn costs change the value of animal search paths. *Ecology Letters*, 16, 1145–1150.

Wilson, R. P., Quintana, F. & Hobson, V. J. (2012). Construction of energy landscapes can clarify the movement and distribution of foraging animals. *Proceedings of the Royal Society B*, 279, 975–980.

Wood, S. N. (2017). *Generalized Additive Models: An Introduction with R*. 2nd edn. Chapman and Hall/CRC.

Appendix A

1 Radius Size, R

To approximate Equation 2, we generate controls on a disc (Section 2.2). By using this approximation method, we therefore assume that the probability density function of a step ending at y given that it started at x over the area of the disc, is

$$f(y|x) = \begin{cases} \text{Eq. } 2 & \text{if } l_{xy} \leq R \\ 0 & \text{if } l_{xy} > R \end{cases} \tag{A.1}$$

Therefore, for this approximation to be accurate, the disc needs to be large enough so that the probability of a step longer than R is very small (Figure A.1). If we define the radius as $R = l_m \times \gamma$, where l_m is the maximum observed step length, the approximation will improve as γ increases. However, as the size of the disc becomes larger, so does the number of controls needed for the approximation. There is no straightforward way to assess this trade-off (i.e., the optimal size of R), but we can use importance sampling, based on where we expect the ESF to take large values. We explore the effect of the size of R on the approximation using simulated data, as well as comparing individual polar bear estimates approximated with different values of γ.

Simulated Data We simulated 250 movement tracks $\{x_1, x_2, \ldots, x_n\}$ of length $n = 250$, as described in Section 3. For each step, we generated 50 controls on a disc with a radius of the size $R = l_m \times \gamma$, where $\gamma = 0.5, 1.1, 2$. We fit the ESF for each movement track. As expected, β_2 was estimated with the lowest precision with the smallest radius ($\gamma = 0.5$). It was estimated correctly when $\gamma \geq 1.1$ (Figure A.2). However, this represents a simplistic example, where the costs are *only* dependent on step length and $\beta_2 = 15$ is fairly strong selection against costs (i.e., the step length distribution should quickly decay to 0).

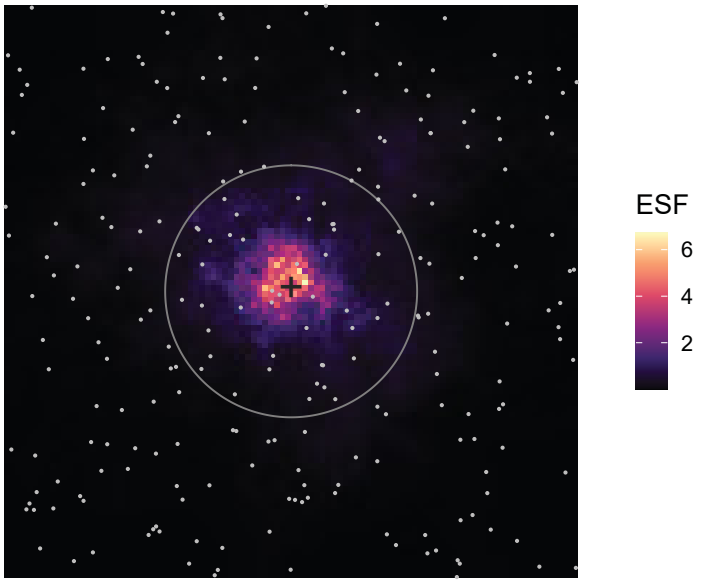

Figure A.1: Plot illustrating importance sampling in the ESF. Theoretically, we should sample uniformly over the entire study area (white dots). However, the ESF should decay with distance from the start point (+), due to the effect of step length on costs, and controls generated outside the disc will contribute very little to the approximation (i.e., their ESF is nearly zero). Therefore, for computational convenience, we can just sample within the disc, as long as the radius is large enough.

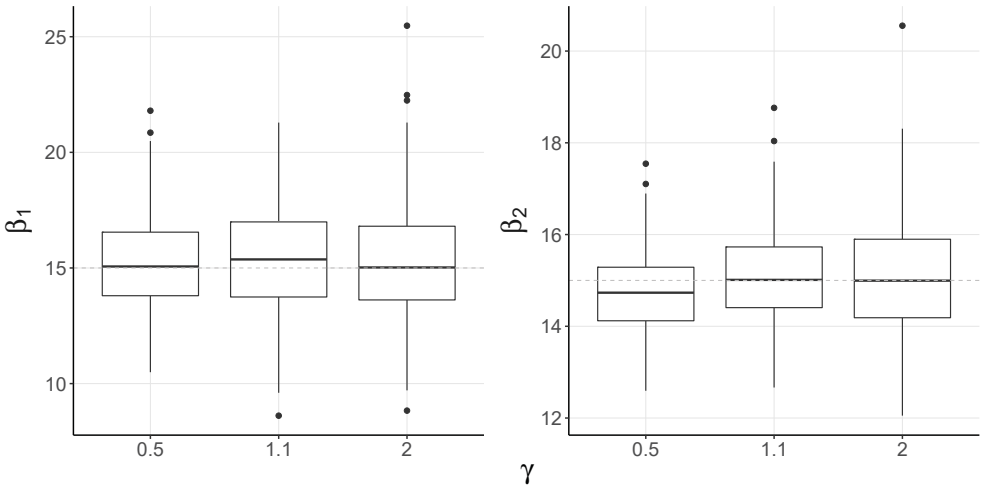

Figure A.2: Estimates of β_1 and β_2 with $R = \gamma \times l_m$, where l_m is the maximum observed step length and $\gamma = 0.5, 1.1, 2$. Dashed line represents the true parameter value.

Real Data We checked the effect of radius size on our polar bear telemetry data. We generated controls on a disc with $R_1 = 1.1 \times l_m$ and $R_2 = 2 \times l_m$ for each individual, fit the models separately, and then compared parameter estimates. Estimates varied up to ± 0.15 for β_2 (Figure A.3), but followed the same general pattern. There was no evidence of systematic bias (i.e., underestimation or overestimation), and variation may be explained by the random generation of controls (which varied between the two trials). β_1 also varied between the two radius sizes, but this is likely attributable to high uncertainty in the estimates (i.e., no clear selection for gains).

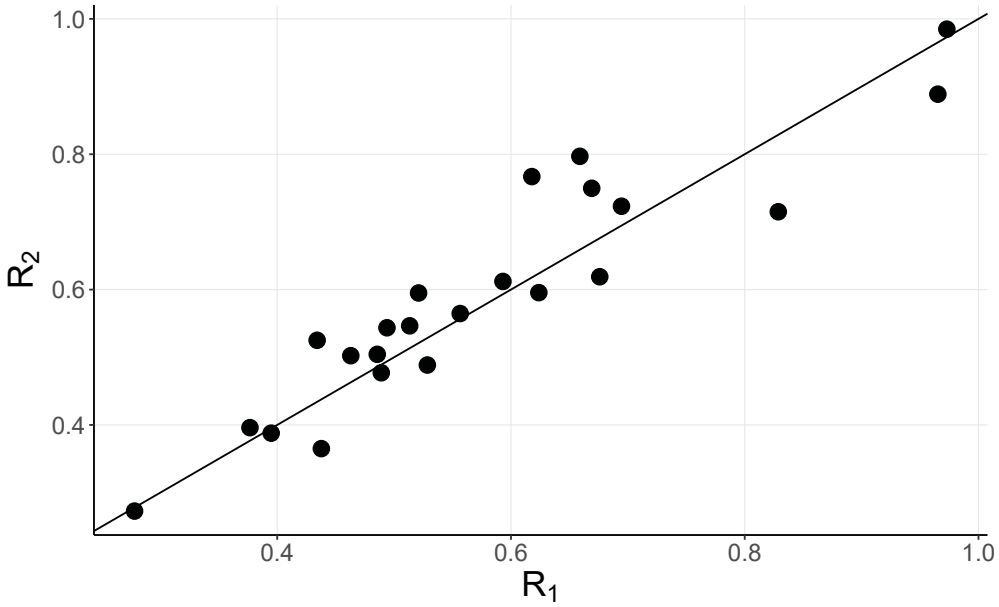

Figure A.3: Individual estimates of β_2 with $R_1 = 1.1 \times l_m$ and $R_2 = 2.0 \times l_m$. Each point is an individual polar bear and the straight line represents a 1:1 relationship.

2 Polar Bear Case Study

2.1 Study Area and Field Sampling

Field sampling was done in Beaufort Sea, Canada (Figure A.4). Sea ice in the area is mostly annual, with a flaw lead that separates near-shore areas of stable landfast ice and off-shore drifting pack ice (Carmack & Macdonald, 2002). The lead widens in spring and forms an active sea ice zone with high productivity (Pilfold *et al.*, 2014), before most ice disappears by mid-summer (Stern & Laidre, 2016). Sea ice drift is characterized by the clockwise Beaufort

Gyre, which is strengthening with climate change (Hutchings & Rigor, 2012; Petty *et al.*, 2016), and increasing the energetic expenditure of polar bears in the area (Durner *et al.*, 2017).

Following standard capture procedures (Stirling *et al.*, 1989), polar bears were sighted and immobilized in April-May of 2007-2011. Bears were fitted with GPS collars (Telonics, Mesa, AZ) set to a collect locations at a 4-hour resolution (relayed via the Argos satellite system; CLS America, Lanham, MD), and programmed to release after 1-2 years. The age of each bear was determined by analysing cementum growth layers of an extracted vestigial premolar (Calvert & Ramsay, 1998), and sex was determined in the field. Capture and handling was approved by the University of Alberta BioSciences Animal Care and Use Committee following guidelines from the Canadian Council on Animal Care.

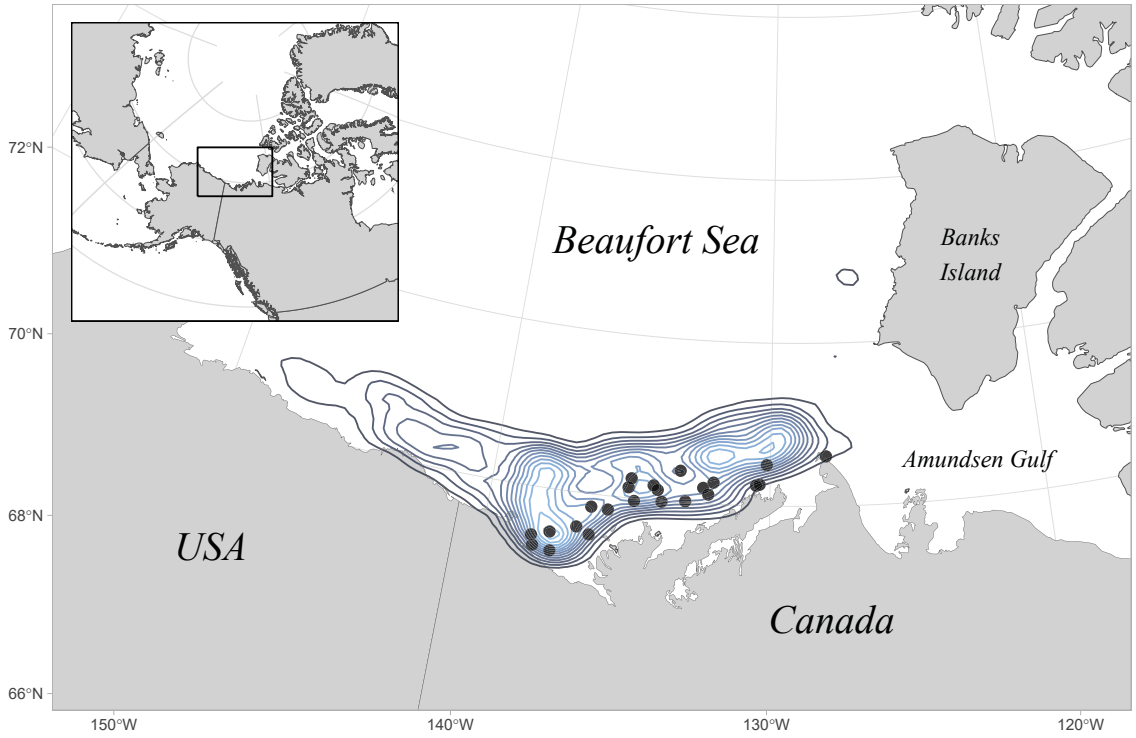

Figure A.4: Study area in the Beaufort Sea, Canada. Circle points are polar bear collar deployment locations, and contour lines show the density of satellite telemetry data for all individuals (once regularised and limited to the spatiotemporal extent of the energetic gains raster).

2.2 Polar Bear Cost Modelling

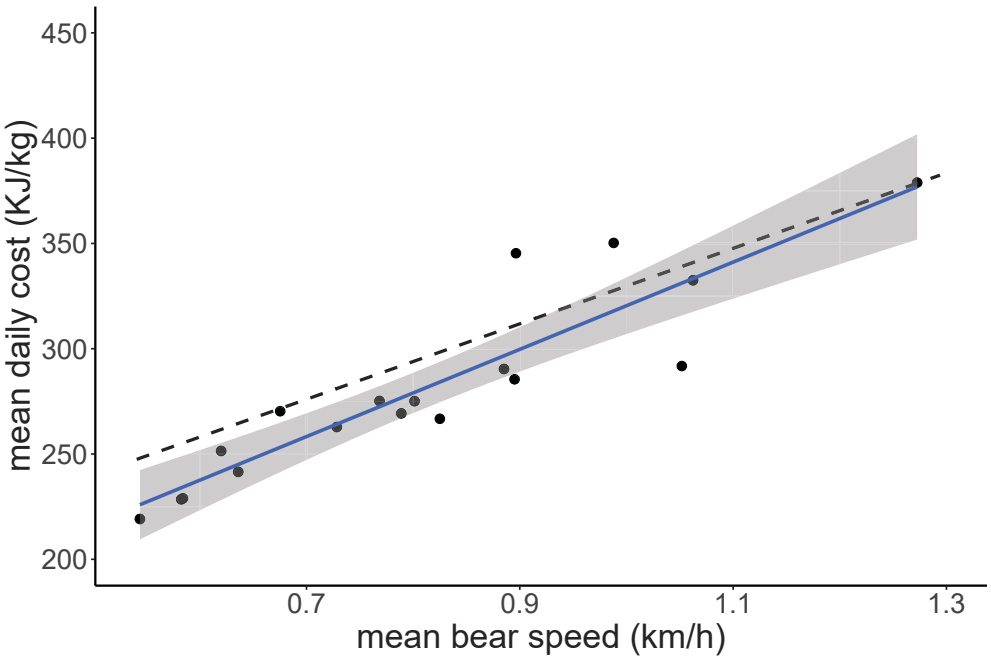

Figure A.5: Relationship between mean daily movement speed (km/h) and daily energy expenditure (kJ/kg) for individuals with more than 25 days of locations with 6 locations (blue line) compared to the estimated relationship from doubly-labelled water (Pagano & Williams, 2019).

2.3 Comparison to a Simple Isotropic Random Walk Model

The simple isotropic random walk (SRW) is unbiased and uncorrelated, with diffusion coefficient D, such that the density of a step starting at x and ending at y over time interval t is normally distributed around the start point: $y \sim N(x, \sigma^2)$, where $\sigma^2 = 4Dt$ (Codling *et al.*, 2008). The likelihood of a step ending at y given that it started at x is $f(y|x) = \psi(y|x, \sigma^2)$, where ψ is the probability density function (PDF) of a normal distribution of y with mean x and variance σ^2.

Model Formulation and Implementation We can write the SRW as a special case of the ESF. The ESF likelihood of a step ending at y given that it started at x is

$$f(y|x) = S^{-1} \exp[\beta_1 G(x, y) - \beta_2 C(x, y)] \tag{A.2}$$

where S^{-1} is a normalization constant that ensures it is a PDF of y. To write it as an SRW, we can set $\beta_1 = 0$ to represent no effect of energetic gains and $C(x, y) = (y - x)^2$. The likelihood then becomes $f(y|x) = S^{-1} \exp[-\beta_2 (y - x)^2]$, which can be rewritten as

$$f(y|x) = S^{-1} \exp\left[-\frac{(y - x)^2}{2\sigma^2}\right] \tag{A.3}$$

where $\beta_2 = \frac{1}{2\sigma^2}$. We recognize this as the PDF of a bivariate normal distribution with variance σ^2, mean x, and $S = 2\pi\sigma^2$. This shows that an ESF with no gains and $C(x, y) = (y - x)^2$ (i.e., costs formulated as the step length squared) is equivalent to an SRW model.

Model Fitting Following Sections 2.2 and 4.1, we fit the SRW separately for each individual using *optim*. Costs were defined as l^2, where l is the ice drift-corrected bear step length (km). We compared models using AIC scores, where $AIC = 2 \times nllk + 2v$ where $nllk$ is the negative log-likelihood and v is the number of parameters in each model ($v_{ESF} = 2$ and $v_{SRW} = 1$).

Results SRW costs ranged from $0 - 509$ km^2 and ESF costs ranged from $3.3 - 161$ MJ. Since costs are in different units between models, β_2 estimates are on different scales (Figure A.6). However, this does not affect the likelihood or AIC scores. The ESF was a better fitting model in almost all cases: $AIC_{ESF} < AIC_{SRW}$ for 20 out of 23 individuals (Figure A.7). Based on guidelines from Burnham & Anderson (2002), there was little to no support for the competing model ($\Delta AIC > 6$) in all but one case (bearID = E; $AIC_{ESF} = -326.3$, $AIC_{SRW} = -325.5$). All but 3 cases had $\Delta AIC > 10$, which indicates essentially no support for the competing model (Burnham & Anderson, 2002).

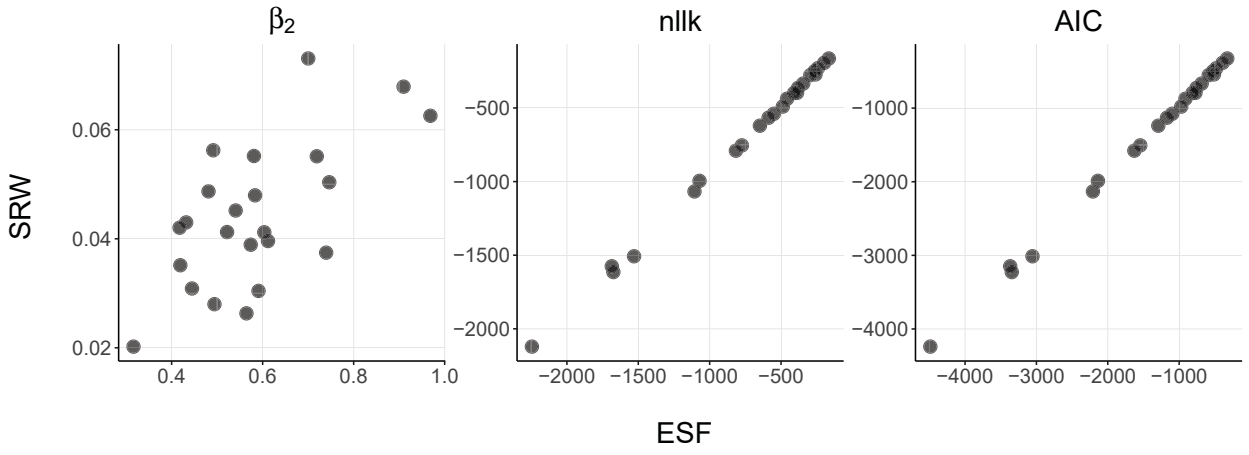

Figure A.6: Parameter (β_2) estimates, negative log-likelihoods (nllk) and AIC scores for the ESF and SRW.

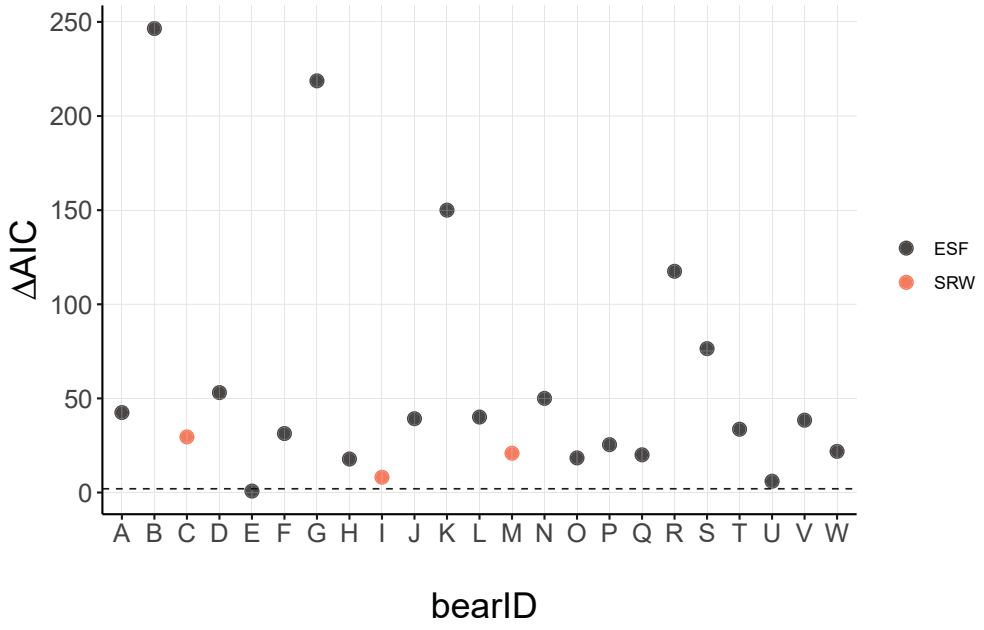

Figure A.7: Comparison of AIC scores for bears with lower AIC_{ESF} (black dots; $\Delta AIC = AIC_{SRW} - AIC_{ESF}$) and lower AIC_{SRW} (red dots; $\Delta AIC = AIC_{ESF} - AIC_{SRW}$). The dashed line is at 2, which is a threshold to indicate considerable support for the model.